Süleyman Demirel Üniversitesi
Fen Bilimleri Enstitüsü Dergisi
Cilt 28, Sayı 3, 348-357, 2024

Süleyman Demirel University
Journal of Natural and Applied Sciences
Volume 28, Issue 3, 348-357, 2024

DOI: 10.19113/sdufenbed.1471672

When Escitalopram is Surrounded by Ethanol: A DFT and QTAIM Approach to Analyze The Drug and The Alcohol Interactions and It's Possible Outcomes

Özge BAĞLAYAN[1*], Mustafa Kemal KARAMAN [2], Cemal PARLAK[3], Özgür ALVER[4]

[1,2,4] Eskişehir Technical University, Science Faculty, Department of Physics, 26470, Eskisehir, Türkiye
[3]Department of Physics, Ege University, Science Faculty, İzmir, 35100, Türkiye

(Alınış / Received: 21.04.2024, Kabul / Accepted: 02.09.2024, Online Yayınlanma / Published Online: 23.12.2024)

Keywords
Escitalopram,
Drug-Alcohol Interaction,
DFT,
QTAIM

Abstract: In the scope of this work the antidepressant escitalopram was surrounded by ethanol commonly referred as alcohol step by step and the possible results of this invasion on escitalopram drug molecule were examined principally by density functional theory methods. Moreover, for analyzing hydrogen bonding interactions, quantum theory of atoms in molecules was used. In this method, the nature of interaction is classified whether it is covalent, partially covalent or noncovalent. According to the results, depending on the interaction edges of the title molecules, it was observed that the escitalopram under attack by ethanol shows quite different interaction characteristics, chemical and electronic properties effecting its chemical reactivity and biological activity which must be taken into account when used together with alcohol.

Essitalopram Etanol ile Çevrelendiğinde: İlaç ve Alkolün Etkileşimlerini ve Olası Sonuçlarını Analiz Etmek için QTAIM ve DFT Yaklaşımı

Anahtar Kelimeler
Essitalopram,
İlaç-Alkol Etkileşimi,
DFT,
QTAIM

Öz: Bu çalışma kapsamında antidepresan essitalopram, yaygın olarak alkol olarak adlandırılan etanol ile adım adım çevrelendi ve bu çevrelemenin essitalopram ilaç molekülü üzerindeki olası sonuçları yoğunluk fonksiyonel teorisi ile incelendi. Ayrıca hidrojen bağı etkileşimlerini analiz etmek için moleküllerdeki atomların kuantum teorisi kullanılmıştır. Bu yöntemde, etkileşimin doğası kovalent, kısmi kovalent veya kovalent olmayan olarak sınıflandırılır. Elde edilen sonuçlara göre etanol ile çevrelenen essitalopramın, alkolle birlikte kullanıldığında dikkate alınması gereken oldukça farklı kimyasal özellikler gösterdiği gözlemlendi.

1. Introduction

The simultaneous use of ethanol (EtOH), also known as alcohol, and medications has been continuously becoming a serious public health concern all over the world [1, 2]. The underlying interaction mechanism between medicines and alcohol is not fully enlightened. However, it is known that pharmacokinetic and pharmacodynamic interactions play an important role [3]. Patients with high rate of alcohol consumptions are considered at high risk of pharmacological interactions since the use of several medications make the pharmacokinetic and pharmacodynamic interferences of ethanol are possible [4]. However, the available data on this subject is rare.

Major depressive disorder is a prevalent mental illness affecting the ever-increasing number of people all around the world [5]. Depression appears as a complex heterogeneous disorder and its pathogenesis includes many factors ranging from genetic to social factors, most of which are not clearly understood [6]. Escitalopram (ESCI) is a selective serotonin reuptake inhibitor and it has been used for the treatment of several disorders such as depression, general anxiety and panic disorder [7, 8]. ESCI is known as a very effective and generally well tolerated drug for the treatment of generalized anxiety problems [9].

Quantum chemical calculations are extensively employed for the examination of the ground state properties of different types of molecular systems in order to understand the chemical process and

*Corresponding author: obaglayan@eskisehir.edu.tr

reactivity of the examined compounds [10-12]. Within the computational applications, density functional theory (DFT) appears as a widely used method offering acceptable accuracy and reliability [13, 14]. It is clear that experimental approaches for biological applications require extensive amount of time on financial resources. At this point computational point of views are very useful to obtain beforehand information to follow more object-oriented pathways for the experimental works. In order to analyze the hydrogen bonding (HB) interactions, quantum theory of atoms in molecules put forward by Bader was used [15]. In QTAIM method by examining the Laplacian of electron density $\nabla^2\rho$ and electronic energy density H, the nature of interaction is classified whether it is covalent, partially covalent or noncovalent [16].

2. Computational Method

First of all, single isolated ESCI and EtOH were optimized. Then NBO charge distributions for ESCI was calculated in order to determine the possible interaction points with EtOH. Four possible interaction sites for ESCI molecule were determined based on NBO charge distributions as seen in Figure 1. Therefore, the sites where partially negative N, O and F atoms are present were selected as active interaction edges. Then for one interaction site one EtOH molecule was brought the nearby interaction point of ESCI and the system was optimized to find the minimum energy configuration. This process was carried out for four interaction sites of ESCI molecule. After this, each time one more EtOH was added to ESCI and the optimization process was carried out for each system which requires many calculations to reach a fully surrounded ESCI by EtOH with stable form of cluster. It is worth noting that for EtOH two possible point groups C_1 and C_s are the case. However, the structure belonging to C_s point group was found lower in energy in magnitude. Henceforth, for all calculations and interactions C_s point group was considered for EtOH. The energies of each hydrogen bond (E_{HB}) were calculated using Espinosa-Molins-Lecomte equation as following [17,18]:

$$E_{HB} = 0.5\ V(rBCP)$$

In the given equation, V(rBCP) is the value of local potential energy density (Virial field) at the bond critical points.

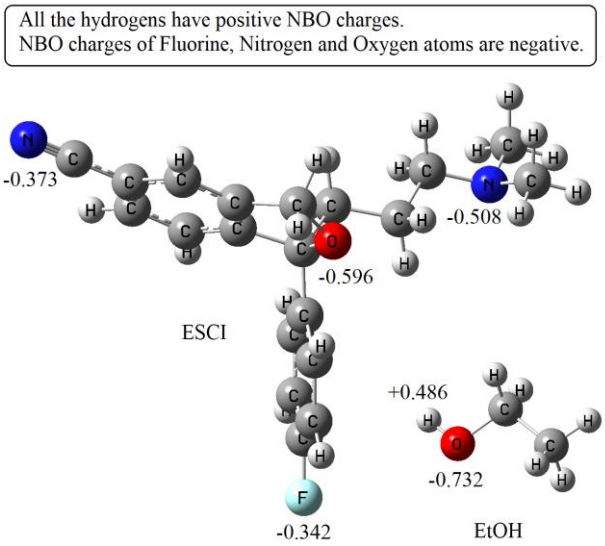

Figure 1. Some important NBO charges and interaction edges of the optimized ESCI and EtOH molecules.

The binding energies (E_b) between EtOH and ESCI drug were calculated by using the following equations:

$(1xEtOH)$:

$E_b = E_{ESCI\&1xEtOH} - (E_{ESCI} + E_{EtOH(site-I,site-II,site-III\ or\ site-IV)} + E_{EtOH})$

$(2xEtOH)\ for\ site-I$:

$E_b = E_{ESCI\&2xEtOH} - (E_{ESCI\&EtOH(site-II)} + E_{EtOH})$

$(2xEtOH)\ for\ site-II$:

$E_b = E_{ESCI\&2xEtOH} - (E_{ESCI\&EtOH(site-I)} + E_{EtOH})$

$(3xEtOH)\ for\ site-I$:

$E_b = E_{ESCI\&3xEtOH} - (E_{ESCI\&EtOH(site-II\&site-III)} + E_{EtOH})$

$(3xEtOH)\ for\ site-II$:

$E_b = E_{ESCI\&3xEtOH} - (E_{ESCI\&EtOH(site-I\&site-III)} + E_{EtOH})$

$(3xEtOH)\ for\ site-III$:

$E_b = E_{ESCI\&3xEtOH} - (E_{ESCI\&EtOH(site-I\&site-II)} + E_{EtOH})$

$(4xEtOH)\ for\ site-I$:

$E_b = E_{ESCI\&4xEtOH} - (E_{ESCI\&EtOH(site-II\&site-III\&site-IV)} + E_{EtOH})$

$(4xEtOH)\ for\ site-II$:

$E_b = E_{ESCI\&4xEtOH} - (E_{ESCI\&EtOH(site-I\&site-III\&site-IV)} + E_{EtOH})$

$(4xEtOH)\ for\ site-III$:

$E_b = E_{ESCI\&4xEtOH} - (E_{ESCI\&EtOH(site-I\&site-II\&site-IV)} + E_{EtOH})$

$(4xEtOH)\ for\ site-IV$:

$E_b = E_{ESCI\&4xEtOH} - (E_{ESCI\&EtOH(site-I\&site-II\&site-III)} + E_{EtOH})$

where all the statements like $E_{ESCI\&1xEtOH}$, $E_{ESCI\&2xEtOH}$, $E_{ESCI\&3xEtOH}$, $E_{ESCI\&4xEtOH}$ present the optimized energies of the related systems. The determination of functionals and the basis sets effects the required computational sources. It is clear that higher level of functionals and basis sets mean long calculation times and robust computational resources which are not available for most of the researchers. In our previous study, we reported that compared with several solvation models, functionals and the basis sets, the B3LYP/6-31G(d) level of theory with the polarizable continuum model enables to get acceptable outcomes compared to higher level of time-consuming

computations [19]. Since water is the most plentiful molecule in biological systems, all calculations were carried out with B3LYP functional along with the 6-31G(d) basis set in water media. During the calculations the interacting atoms within a molecular system approach each other, henceforth, their basis functions overlay. This effect is named as basis set superposition error (BSSE). In order to eliminate or to reduce the BSSE effect, the counterpoise correction method was used [20]. Calculations were carried out with Gaussian 09 program package [21]. GaussView was used for the creation of molecular structures and visualization of molecular orbitals [22]. QTAIM computations were performed using the Multiwfn program [23].

3. Results

3.1. ESCI vs 1xEtOH, site-I to site-IV ınteractions

In this part of the work four interaction sites were identified and one EtOH molecule interacted with identified sites named as Site-I, Site-II, Site-III and Site-IV. The optimized structures were given in Fig. 2. For the structures S1, S2, S3 and S4, the O—H…N≡C, O—H…N, O—H…O and O—H…F interatomic distances were calculated as 1.990, 1.864, 1.901 and 2.019 Å, respectively which indicates the requirements for structurally stable interaction distances depending on the atomic radii and partial charges at the interaction edges. The OH stretching/bending vibrations of single isolated EtOH molecule were calculated as 3745/1479 cm^{-1}. As for the interacted structures S1, S2, S3 and S4 OH stretching/bending vibrations were computed as 3645/1492, 3284/1530, 3610/1491 and 3737/1481 cm^{-1}, correspondingly. It is clear that OH stretching vibrations were red shifted in the IR spectra. On the other hand, OH bending vibrations showed blue shifts in the IR spectra. While the largest red shift in the IR spectrum was observed for S2 structure with a value of 461 cm^{-1}, the smallest red shift was found for S4 system with a value of 8 cm^{-1}. This fact suggests that with an IR instrument having a typical resolution of 2 cm^{-1}, both shifts are observable and distinguishable. In the same way, while the largest blue shift in the IR spectrum was found for S2 structure with a value of 51 cm^{-1}, the smallest blue shift was observed for S4 system with a value of 2 cm^{-1}. It is worth noting that the largest and smallest shifts of OH vibrational and bending bands occur where the interatomic distances at the interaction sites are the smallest and the largest, correspondingly.

The BSSE uncorrected/corrected E_b energies were calculated as -4.17/-2.94 (Site-I), -8.48/-5.07 (Site-II), -6.19/-2.34 (Site-III) and -4.14/-0.51 kcal/mol (Site-IV). It is seen that while the strongest interaction occurs at Site-II, the weakest interaction occurs at Site-IV. It is seen that upon BSSE correction E_b values tend to change by 29% (Site-I), 40% (Site-II), 62% (Site-III) and 88% (Site-IV). The corrections appear at quite high particularly where the E_b energy is smallest in magnitude, therefore, for the possible studies carried out at B3LYP/6-31G(d) level of theory this correction is suggested to be considered.

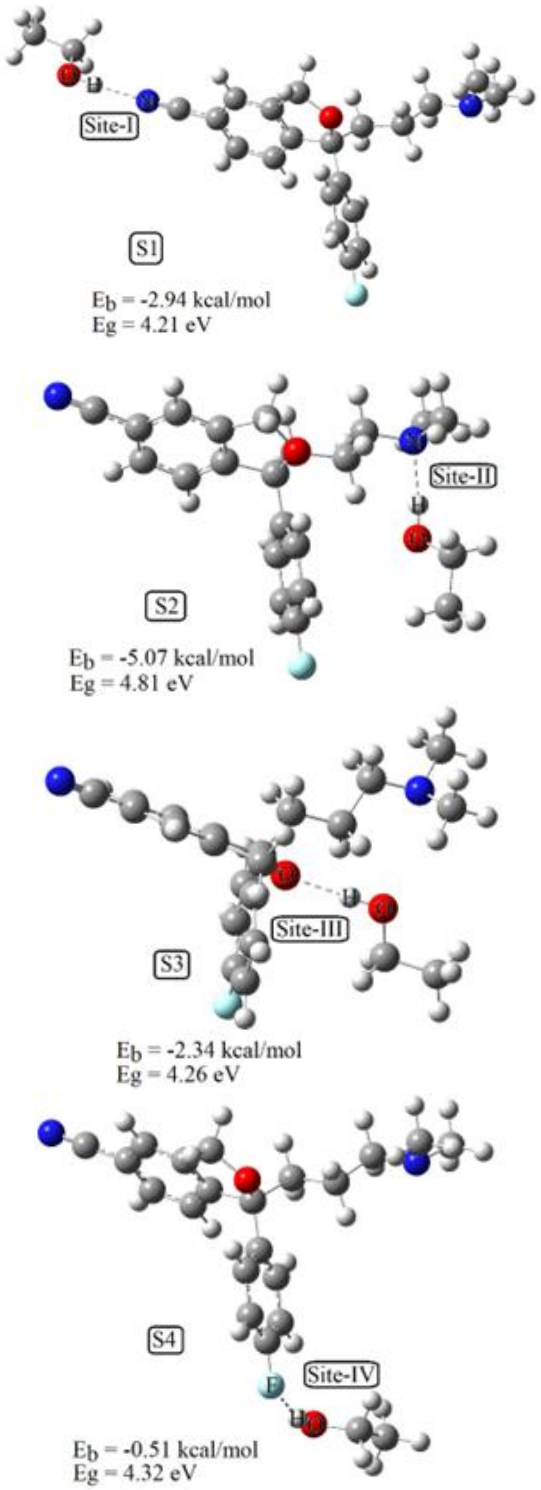

Figure 2. Optimized structures of the single EtOH interacted systems.

The HOMO-LUMO, E_g value of single isolated ESCI was calculated as 4.33 eV. The E_g value is considered as a measure of reactivity for a given molecular system [24]. Therefore, it can be concluded that as for Site-I, Site-III and Site-IV interactions reactivities of the interacted systems increase more or less but as for Site-II interacted system reactivity decreases compared to single isolated ESCI drug molecule (Fig. 2). It is seen that each interaction site tends to produce different reactivity conditions. At this point, it is worth noting that the comparison of the reactivity was carried out between single ESCI and ESCI interacted EtOH system rather than isolated single molecules.

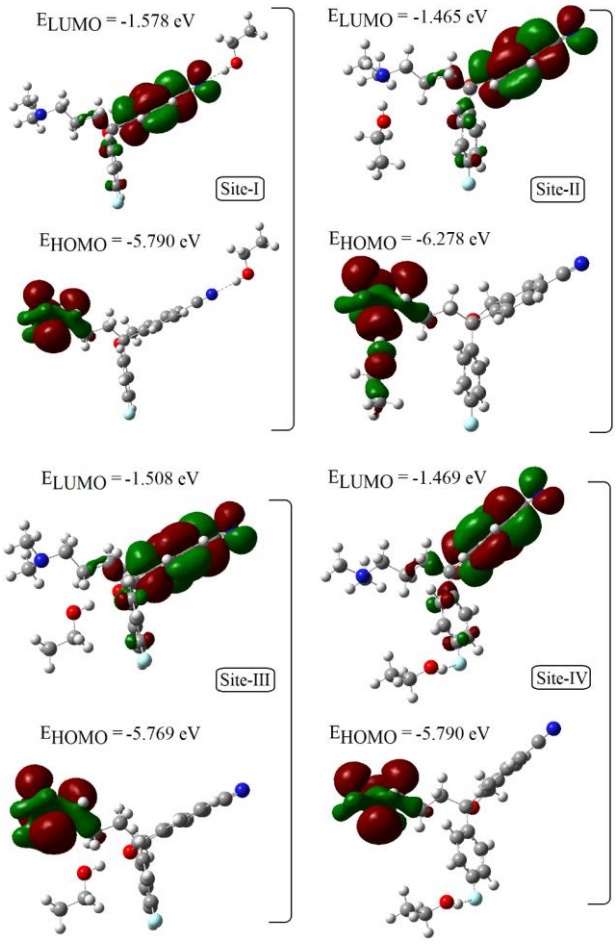

Figure 3. Frontier molecular orbital maps for 1xEtOH interacted systems.

The HOMO-LUMO maps for any molecular system can be considered as a tool to identify the regions where the probability of electron donation and acceptance are high [25]. Frontier molecular orbitals are given in Fig. 3. For Site-I-IV interactions LUMOs are distributed over ESCI drug molecule. No matter which site the interaction occurs, LUMOs are only located over ESCI. Therefore, it can be drawn that the probability of ESCI fragments of the interacting systems behaving as electron acceptors are higher when compared to EtOH. In addition to that, electron affinity (EA) is known as $-E_{LUMO}$ [26] which means that EA values of the interacted systems mainly determined by the ESCI drug molecule. HOMOs like LUMOs are distributes mainly over ESCI only one exception which is Site-II interaction. For Site-II interaction HOMOs are located on EtOH and ESCI molecules at the same time. At this point, it is worth noting that HOMO-LUMO distributions indicate regions where electron transitions are most likely to occur. Therefore, EtOH can also donate electrons for Site-II type of interaction in addition to ESCI. Since ionization potential (IP) is known as $-E_{HOMO}$ [26], it seen that IP and EA values show dependence at the interaction sites and as can be seen in Fig. 2 and Fig. 3. While S2 structure has the highest IP, S3 has the lowest IP. Further, while the S1 shows the highest EA, S2 has the lowest EA.

3.2. ESCI vs 2xEtOH, the multiple site-I and site-II interactions

In this part of the study, a situation in which Site-I and Site-II parts of ESCI interact with EtOH compounds simultaneously was examined. The optimized structure was shown in Fig. 4. The calculated O—H...N≡C and O—H...N interatomic distances were calculated as 1.990 and 1.869 Å, respectively. The OH stretching vibrations were computed as 3646 (Site-I) and 3290 cm^{-1} (Site-II) for the examined system. OH bending vibrations do not change compared to single EtOH interacted ESCI and they appeared at 1492 (Site-I) and 1530 cm^{-1} (Site-II). The BSSE uncorrected/corrected E_b energies were found as -4.22/-2.99 (Site-I) and -8.54/-5.02 kcal/mol (Site-II). It is seen that the strongest interaction occurs at still Site-II. Compared to single EtOH interacted systems, 2xEtOH interaction leads an increase for E_b energies in magnitude. EtOH molecules more strongly interacted for 2xEtOH system. Therefore, stability of system seems sensitive to the number of interacted EtOH molecules. E_g value of 2xEtOH interacted system was calculated as 4.70 eV. It is seen that reactivity of 2xEtOH interacted system is less than ESCI alone.

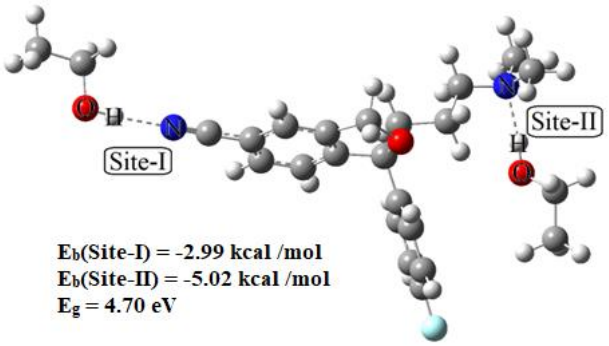

Figure 4. Optimized structures of the 2xEtOH interacted system.

Frontier molecular orbitals for 2xEtOH interacted system are given in Fig. 5. It is seen that LUMOs are

distributed over ESCI and HOMOs are distributed both ESCI and EtOH molecules. Therefore, for 2xEtOH interacted system while only ESCI shows a high probability as an electron acceptor, both ESCI and (Site-II) EtOH possess potentials as electron donors. The EA value of the 2xEtOH interacted system was found as 1.580 eV (Fig. 5) which is higher than the values obtained for the single EtOH interacted systems.

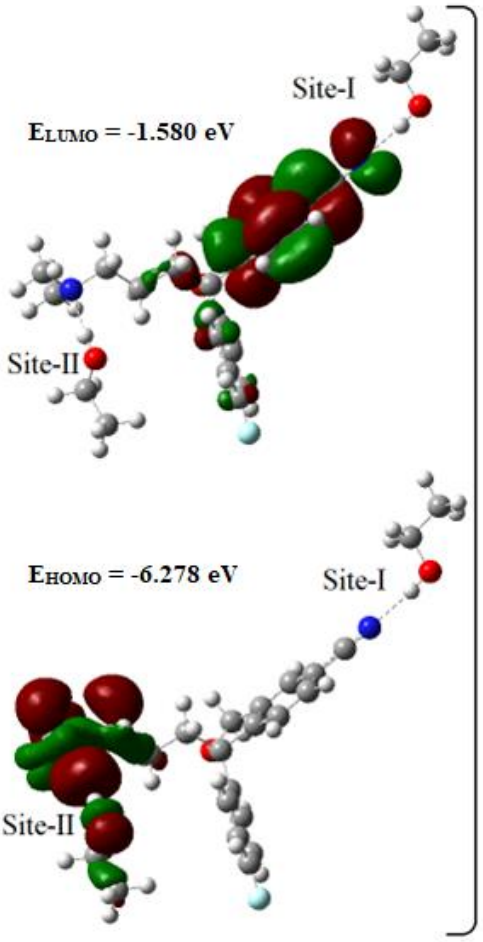

Figure 5. Frontier molecular orbital maps for 2xEtOH interacted ESCI system.

3.3. ESCI vs 3xEtOH, the multiple site-I, site-II and site-III Interactions

In this part of the work one EtOH molecule interacted with the Site-I, Site-II and Site-III simultaneously. The optimized structure was presented in Fig. 6. The calculated O—H…N≡C, O—H…N and O—H…O interatomic distances were calculated as 1.991, 1.869 and 1.901 Å, respectively. The OH stretching vibrations were computed as 3647 (Site-I), 3287 (Site-II) and 3611 cm^{-1} (Site-III) for the investigated system. OH bending vibrations appeared at 1492 (Site-I), 1530 (Site-II) and 1489 cm^{-1} (Site-III). The BSSE uncorrected/corrected E_b energies were calculated as -4.16/-2.95 (Site-I), -8.56/-4.98 (Site-II) and -6.24/-2.31 kcal/mol (Site-III). In this configuration additional EtOH at the Site-III, compared to 2xEtOH system leads changes for E_b energies. The interaction strength at Site-I and Site-II decreases in magnitude slightly. E_g value of 3xEtOH interacted system was computed as 4.63 eV. It is seen that reactivity of 3xEtOH interacted system is still less than ESCI alone.

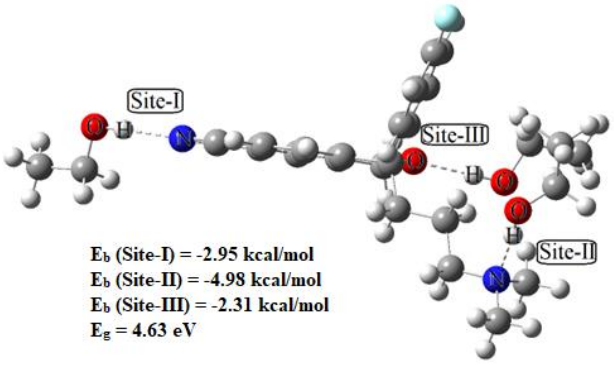

Figure 6. Optimized structures of the 3xEtOH interacted system.

Frontier molecular orbitals for 3xEtOH interacted system are given in Fig. 7. It is seen that LUMOs are distributed only over ESCI and HOMOs are distributed both ESCI and (Site-II) EtOH molecules. In here, unlike Site-II EtOH, Site-I and Site-III interacted EtOH molecules do not tend to accept or donate electrons. The EA value of the 3xEtOH interacted system was found as 1.626 eV (Fig. 7) which is higher than the values obtained for 1xEtOH and 2xEtOH interacted systems.

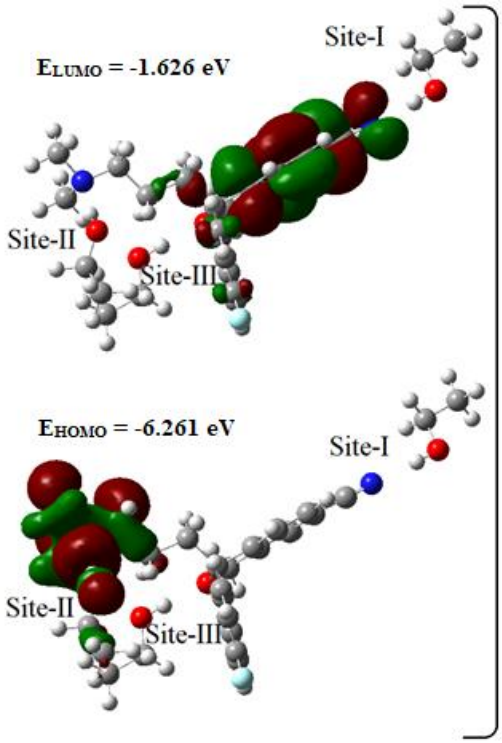

Figure 7. Frontier molecular orbital maps for 3xEtOH interacted ESCI system.

3.4. ESCI vs 4xEtOH, the multiple site-I, site-II, site-III and site-IV Interactions

In here one EtOH molecule interacted with the Site-I, Site-II, Site-III and Site-IV simultaneously. The optimized structure was given in Fig. 8. The calculated O—H…N≡C, O—H…N, O—H…O and O—H…F interatomic distances were found as 1.992, 1.868, 1.906 and 2.024 Å, respectively. The OH stretching vibrations were determined as 3647 (Site-I), 3286 (Site-II), 3610 (Site-III) and 3741 cm^{-1} (Site-IV) for the investigated system. At this point it is seen that infrared vibrational bands at the interaction sites show changes around 2-4 cm^{-1}, when compared to single EtOH interactions with ESCI drug molecule which means that nearly similar diagnostic IR bands observed for 1xEtOH interacted ESCI and 4xEtOH interacted ESCI systems. OH bending vibrations appeared at 1492 (Site-I), 1530 (Site-II), 1490 (Site-III) and 1482 cm^{-1} (Site-IV). It appears that OH bending vibrations are less effected compared to OH stretching vibrations upon interaction with ESCI drug molecule. The BSSE uncorrected/corrected E_b energies were calculated as -4.16/-2.95 (Site-I), -8.58/-4.91 (Site-II), -6.15/-2.21 (Site-III) and -4.10-/0.41 kcal/mol (Site-IV). E_g value of 4xEtOH interacted system was computed as 4.63 eV which is the same value with 3xEtOH interacted system and reactivity of 4xEtOH interacted system is still stays below than ESCI alone.

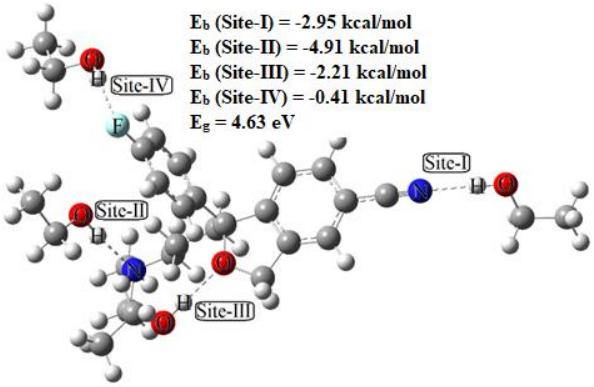

Figure 8. Optimized structures of the 4xEtOH interacted system.

In Fig. 9, IR spectra of selected regions of ESCI and ESCI interacted 4xEtOH molecule were given. It is clear that following the EtOH interaction with ESCI drug relative intensity of C≡N stretching vibration considerably decreases due to redistribution of charges at the interaction sites or changes of the polarity of C≡N bond. The OH stretching vibrations can also be followed in Fig. 9.

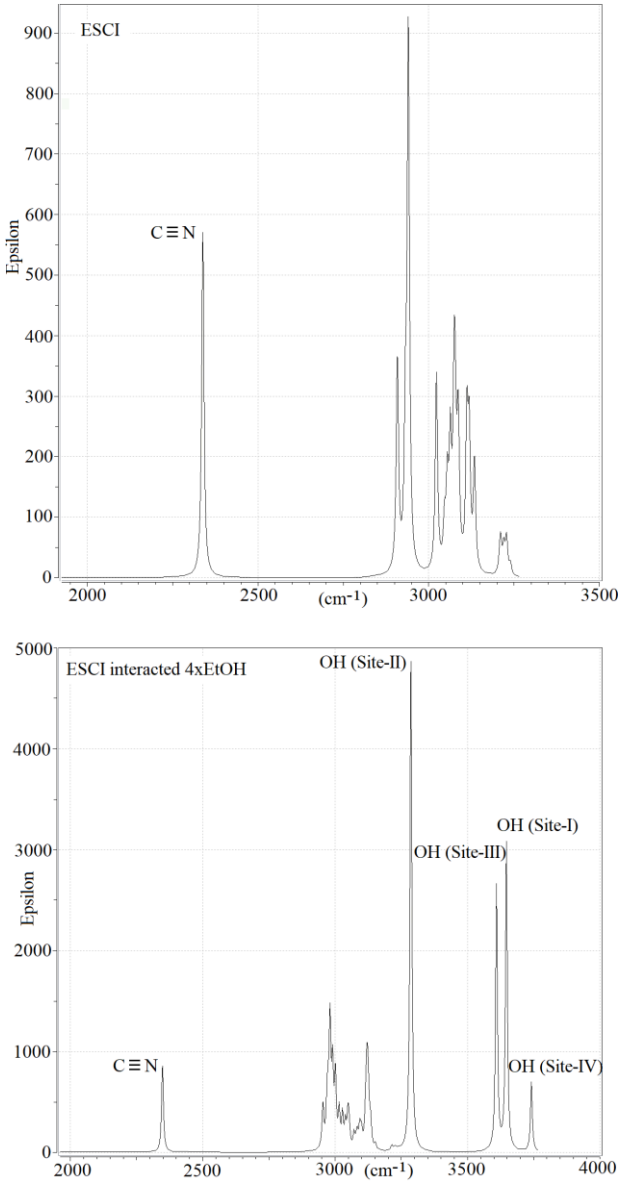

Figure 9. Selected region of calculated IR spectra of ESCI and ESCI interacted 4xEtOH

NBO charge distributions at the interaction sites were also calculated as given in Fig. 10. The NBO charges of oxygen and hydrogen atoms at the interaction site of single isolated EtOH were calculated as -0.732 and +0.486. It was observed that following the interaction with ESCI molecule some number of electrons move towards the oxygen atom of EtOH and as for site-II this flow is more apparent when compared to other sites of interaction resulting with more intense OH stretching band for site-II interaction (Fig. 9). It was seen that the strength of E_b interaction energy is correlated not only the partial NBO charges but also the distance between the interacting atoms.

Frontier molecular orbitals for 4xEtOH interacted system are given in Fig. 11. It is seen that LUMOs are distributed only over ESCI and HOMOs are distributed both ESCI and (Site-II and Site-III) partially EtOH

molecules. It is seen that particularly HOMO distributions of the interacted system having a close relation with electronic properties tend to change depending on the number of interacted EtOH molecule so the electronic properties. As the number of interacted EtOH molecule increases the distributions of electrons over the surface of ESCI molecule show alterations which refers that depending on the interaction site and the number of interacted EtOH molecules, the chemical properties of the examined system can be manipulated. The EA value of the 2xEtOH interacted system was found as 1.630 eV (Fig. 11) which is higher than the values obtained for the 1xEtOH, 2xEtOH and 3xEtOH interacted systems. In general, it was observed that as the number of interacted EtOH increases the EA values also increased. A summary of energetic parameters for comparison can be seen in Table 1.

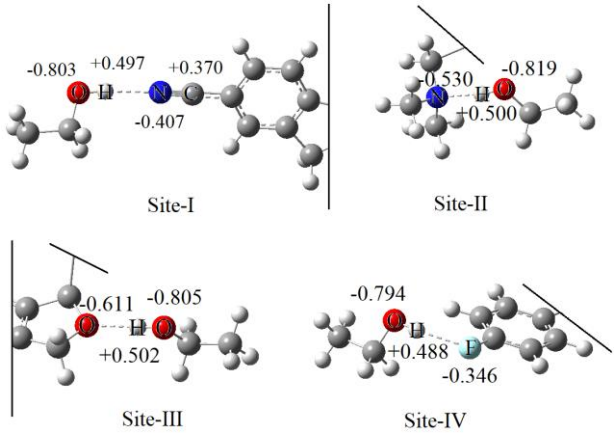

Figure 10. NBO charges at interaction sites

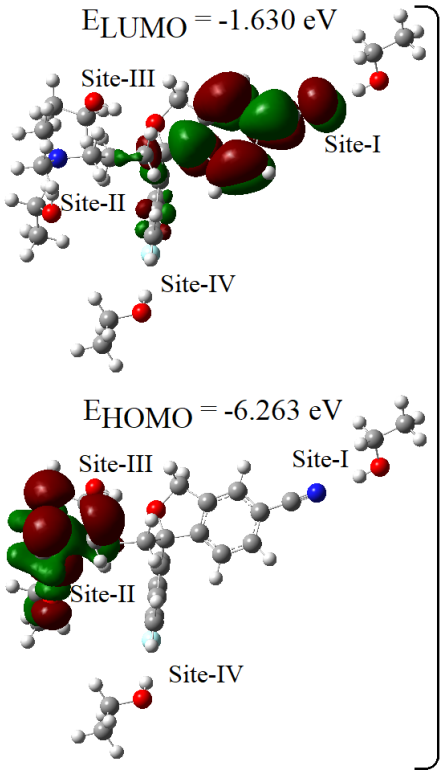

Figure 11. Frontier molecular orbital maps for 4xEtOH interacted ESCI system.

Table 1. A summary of energetic parameters for comparison

Examined systems	E_b (kcal/mol)	E_{HOMO} (eV)	E_{LUMO} (eV)	E_g (eV)
1xEtOH (Site-I)	-2.94	-5.790	-1.578	4.21
1xEtOH (Site-II)	-5.07	-6.278	-1.465	4.81
1xEtOH (Site-III)	-2.34	-5.769	-1.508	4.26
1xEtOH (Site-IV)	-0.51	-5.790	-1.469	4.32
2xEtOH (Site-I)	-2.99	-6.278	-1.580	4.70
2xEtOH (Site-II)	-5.02			
3xEtOH (Site-I)	-2.95			
3xEtOH (Site-II)	-4.98	-6.261	-1.626	4.63
3xEtOH (Site-III)	-2.31			
4xEtOH (Site-I)	-2.95			
4xEtOH (Site-II)	-4.91	-6.263	-1.630	4.63
4xEtOH (Site-III)	-2.21			
4xEtOH (Site-IV)	-0.41			
ESCI	-	-5.788	-1.461	4.33

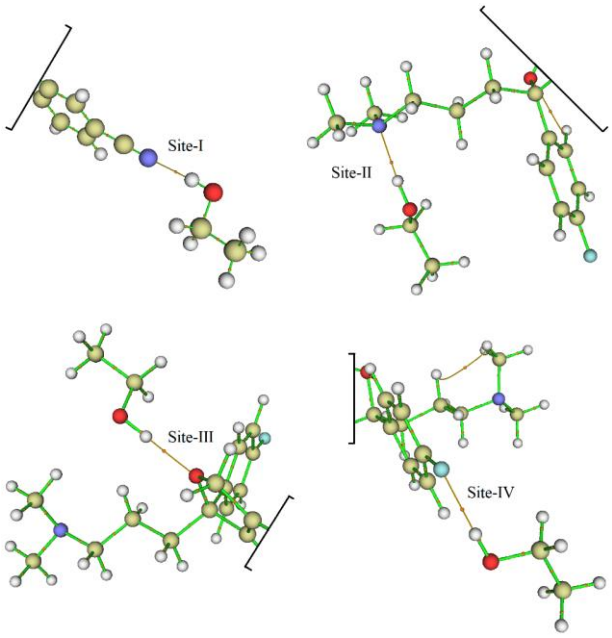

Figure 12. Molecular topographic maps at the interaction sites (the electron density at bond critical points is depicted as orange spheres).

At this point it seems useful to discuss the QTAIM parameters to enlighten the nature of interaction (Table 2 and Fig. 12). For Site-I interaction, electron density ρ, Laplacian electron density $\nabla^2\rho$, and electronic energy density H in atomic units were calculated as 0.025, 0.080 and 0.240 ($x10^{-3}$) which refers an E_{HB} energy of -6.09 kcal/mol. Further, both positive $\nabla^2\rho$ and H values refer that the interaction is noncovalent in nature. As for Site-II interaction, ρ, $\nabla^2\rho$, and H values were calculated as 0.040, 0.096 and -3.47 ($x10^{-3}$) with an E_{HB} energy of -9.73 kcal/mol. Positive $\nabla^2\rho$ and negative H values imply that the interaction is partially covalent in nature. For Site-III interaction, ρ, $\nabla^2\rho$, and H values were found as 0.029, 0.088 and -1.23 ($x10^{-3}$) with an E_{HB} energy of -7.68 kcal/mol. Again, here like Site-II interaction positive $\nabla^2\rho$ and negative H values indicate that the interaction is partially covalent in nature for Site-III interacted system. Finally, as for Site-IV interaction ρ, $\nabla^2\rho$, and H values were found as 0.019, 0.068 and -0.74 ($x10^{-3}$) with an E_{HB} energy of -5.76 kcal/mol referring a partially covalent interaction.

Table 2. Some important QTAIM parameters of 4xEtOH interacted ESCI system.

4xEtOH	ρ(r) (a.u.)	$\nabla^2\rho$(r) (a.u.)	H(r)x10^{-3} (a.u.)	E_{HB} (kcal/mol)
Site-I	0.025	0.080	0.240	-6.09
Site-II	0.040	0.096	-3.47	-9.73
Site-III	0.029	0.088	-1.23	-7.68
Site-IV	0.019	0.068	-0.74	-5.76

4. Discussion and Conclusion

In the framework of this study, an extensive DFT investigation of ESCI interacted EtOH were carried out based on mainly DFT and QTAIM approaches. Structural stabilities of the examined systems were evaluated particularly regarding the binding energies of the interacted systems. Further, electronic properties and some important diagnostic vibrational bands were discussed. In summary following results can be summed up:

I. Electron acceptance or donation properties referred also as HOMO-LUMOs of ESCI drug molecule show dependence in which site the interaction with EtOH occurs. Likewise, it was observed that the interaction energy or the strength of the interaction between ESCI and EtOH changes depend on the interaction site of ESCI molecule.

II. It was found that as the number of interacted EtOH increases, electron affinity of the system increases. Therefore, the number of available interaction site of ESCI plays an important role for determining chemical properties of the examined systems.

III. It was seen that E_g or reactivity characteristics of ESCI drug strongly depends on the interaction site and the number of interacted EtOH molecule which indicates that the chemistry or biological activity of ESCI is affected by the presence of EtOH.

IV. QTAIM results indicate that partially covalent and noncovalent interactions are possible between EtOH and ESCI drug molecule.

Acknowledgment

Authors acknowledge FenCluster System of Ege University for the calculations. This study was supported by the Scientific and Technological Research Council of Turkey (TUBITAK) BİDEB 2209-A Grant No 1919B012302888 and Eskişehir Technical University Scientific Research Projects Commission under grant no 24LÖP001.

Declaration of Ethical Code

In this study, we undertake that all the rules required to be followed within the scope of the "Higher Education Institutions Scientific Research and Publication Ethics Directive" are complied with, and that none of the actions stated under the heading "Actions Against Scientific Research and Publication Ethics" are not carried out.

References

[1] Peacock A., Leung J., Larney S. 2018. Global Statistics on Alcohol, Tobacco and Illicit Drug Use: 2017 Status Report. Addiction, 113, 1905-1926.

[2] Kaufman, E., 1976. The Abuse of Multiple Drugs. I.Definition, Classification, and Extend of Problem. The American Journal of Drug and Alcohol Abuse, 3, 279-292.

[3] Singh, A. 2021. Interaction of Alcohol with Drugs of Abuse and Medicines. Neurobiology of Alcohol and Brain. Academic Press, 75-140.

[4] Guerzoni, S., Pellesi, L., Pini, L.A., Captuo, F. 2018. Drug-drug interactions in the treatment for alcohol use disorders: A comprehensive review. Pharmacological Research, 133, 65-76.

[5] Zheng, P., Wang, Y., Chen, L., Yang, D., Meng, H., Zhou, D., Zhong, J., Lei, Y., Melgiri N.D., Xie, P. 2013. Identification and Validation of Urinary Metabolite Biomarkers for Major Depressive Disorder. Molecular & Cellular Proteomics, 12 (1), 207-214.

[6] Chirit, A.L., Gheorman, V., Bondari, D., Rogoveanu, I. 2015. Current Understanding of The Neurobiology of Major Mepressive Disorder. Romanian Journal of Morphology and Embryology, 56(2 Suppl), 651-658.

[7] Owens, M.J., Knight, D.L., Nemeroff, C.B. 2001. Second-generation SSRIs:human monoamine transporter binding profile of escitalopram and R-fluoxetine. Biological Psychiatry, 50, 345-350.

[8] Jonathan, R.T., Davidson, M.D., Bose A., Korotzer, A., Zheng, H. 2004. Escitalopram in the treatment of generalized anxiety disorder: double-blind, placebo controlled, flexible-dose study. Depression and Anxiety, 19, 234-240.

[9] Dhillon, S., Scott, L.J., Plosker, G.L. 2006. Escitalopram A Review of its Use in the Management of Anxiety Disorders. CNS Drugs, 20, 763-790.

[10] Omurtag Özgen P.S., Durmaz H., Parlak C., Alver Ö., Bağlayan Ö. 2020. Non-covalent functionalization of single walled carbon nanotubes with pyrene pendant polyester: A DFT supported study. Journal of Molecular Structure, 1209, 127943.

[11] Parlak, C., Tepe, M., Bağlayan, Ö., Alver, Ö. 2020 Investigation of detection and adsorption properties of β-propiolactone with silicon and aluminum doped fullerene C_{60} using density functional theory. Journal of Molecular Structure, 1217, 128346.

[12] Parlak, C., Alver, Ö., Bağlayan, Ö. 2021. Quantum mechanical simulation of Molnupiravir drug interaction with Si-doped C_{60} fullerene. Computational and Theoretical Chemistry, 1202, 113336.

[13] Afzal, Q.Q., Rafique, J., Jaffar, K., Perveen, M., Iqbal, J., Al-Buriahi, M.S., Alomairy, S., Alrowaili, Z.A., Somaily, H.H. 2022. DFT study of 2D graphitic carbon nitride based preferential targeted delivery of levosimendan, a cardiovascular drug. Computational and Theoretical Chemistry, 1209, 113584.

[14] Ramana, P. V., Sundius, T., Muthu, S., Mouli, K. C., Krishna, Y. R., Prasad, K. V., Devi, R. N., Irfan, A., Santhamma, C., 2022. Spectroscopic, quantum mechanical, electronic excitation properties (Ethanol solvent), DFT investigations and molecular docking analysis of an anti-cancer drug Bendamustine. Journal of Molecular Structure, 1253, 132211.

[15] R.F.W. Bader. 1990. Atoms in Molecules: A Quantum Theory, Clarendon, New York.

[16] Rozas, I., Alkorta, I., Elguero, J. 2000. Behavior of ylides containing N, O, and C atoms as hydrogen bond acceptors. Journal of the American Chemical Society, 122, 11154–11161.

[17] Espinosa, E., Molins, E., Lecomte, C. 1998. Hydrogen bond strengths revealed by topological analyses of experimentally observed electron densities. Chemical Physics Letters, 285, 170–173.

[18] Mata, I., Alkorta, I., Espinosa, E., Molins, E. 2011. Relationships between interaction energy, intermolecular distance and electron density properties in hydrogen bonded complexes under external electric fields. Chemical Physics Letters, 507, 185–189.

[19] Parlak, C., Alver, Ö., Bağlayan, Ö., Ramasami, P. 2022. Theoretical insights of the drug-drug interaction between favipiravir and ibuprofen: a DFT, QTAIM and drug-likeness investigation. Journal of Biomolecular Structure and Dynamics, 41, 10, 4313–4320.

[20] Gutowski, M., Chalasinski, G. 1993. Critical evaluation of some computational ap- proaches

to the problem of basis set superposition error, The Journal of Chemical Physics, 98, 5540–5554.

[21] Frisch, M. J., Trucks, G. W., Schlegel, H. B. et al. 2016. Gaussian 16, Revision C.01, Gaussian Inc., Wallingford, CT.

[22] Dennington, R.D., Keith, T.A., Millam, J.M., 2016. GaussView 6.0.16, Gaussian Inc.

[23] Lu, T., Chen, F. 2012. Multiwfn: A multifunctional wavefunction analyser, Journal of Computational Chemistry, 33, 580–592.

[24] Suliman, F. O., Al-Nafai, I., Al-Busafi, S. N. 2014. Synthesis, characterization and DFT calculation of 4-fluorophenyl substituted tris(8-hydroxyquinoline)aluminum(III) complexes. Spectrochimica acta. Part A, Molecular and Biomolecular Spectroscopy, 118, 66–72.

[25] Frenking, G., Shaik, S. 2014. The chemical bond. Wiley-VCH, Weinheim, Germany.

[26] Antony Danish, I., Jebasingh Kores, J., Sasitha, T., Winfred Jebaraj, J. 2021. DFT, NBO, HOMO-LUMO, NCI, stability, Fukui function and hole – Electron analyses of tolcapone. Computational and Theoretical Chemistry, 1202, 113296.